Description of a New Blind and Rare Species of Xyliphius (Siluriformes: Aspredinidae) from the Amazon Basin Using High-Resolution Computed Tomography

Authors: Carvalho, Tiago P., Reis, Roberto E., and Sabaj, Mark H.

Source: Copeia, 105(1) : 14-28

Published By: The American Society of Ichthyologists and Herpetologists

URL: https://doi.org/10.1643/CI-16-456

Description of a New Blind and Rare Species of *Xyliphius* (Siluriformes: Aspredinidae) from the Amazon Basin Using High-Resolution Computed Tomography

Tiago P. Carvalho[1,2], Roberto E. Reis[3], and Mark H. Sabaj[2]

***Xyliphius sofiae,* new species, is described based on a unique specimen exhibiting four autapomorphies: eyes absent vs. present (though reduced); color pale, lacking pigment vs. head and body darkly pigmented; branchiostegal rays five vs. four; and unculiferous tubercles on posterior body distributed evenly vs. enlarged unculiferous tubercles typically arranged in five distinct rows above pelvic-fin base to posterior end of caudal peduncle. In addition, the pectoral fin of *X. sofiae,* new species, has one ossified proximal radial vs. two in congeners (except *X. magdalenae,* not examined). *Xyliphius sofiae,* new species, differs from all congeners except *X. lepturus* by snout tip elongated and narrowly rounded vs. short and broadly rounded, often with small median notch; fifth ceratobranchial relatively narrow with elongate acicular teeth vs. broadly expanded, leaf-shaped, with shorter and broader, conical teeth; anterior limits of branchial apertures separated by distance less than length of aperture vs. greater than length of aperture; anal-fin rays modally nine vs. seven; and lateral line extending onto base of caudal-fin rays vs. finishing in hypural region. Based on the single specimen collected in the main channel of the Río Amazonas near Iquitos, Peru, we describe the osteology of *X. sofiae,* new species, using a non-invasive technique: high-resolution X-ray computed tomography (HRXCT). We consider *Xyliphius lombarderoi* Risso and Risso, 1964, a species based on a unique holotype that is now lost, to be a subjective junior synonym of *X. barbatus* Alonso de Arámburu and Arámburu, 1962. Variable characteristics are summarized for the seven species of *Xyliphius* treated here as valid, and their distributions are plotted based on a comprehensive review of museum specimens.**

Se describe la especie nueva *Xyliphius sofiae* basado en un único ejemplar que exhibe cuatro autoapomorfias: ojos ausentes vs. presente (aunque muy reducidos); color pálido, ausencia de pigmento vs. cabeza y cuerpo con pigmentación oscura; cinco radios branquiostegales vs. cuatro; y tubérculos en la parte posterior del cuerpo distribuidos uniformemente vs. tubérculos dispuestas típicamente en cinco filas visibles sobre la región entre la base de la aleta pélvica hasta el pedúnculo caudal. Además, la aleta pectoral de *X. sofiae* tiene un radial proximal osificado vs dos en sus otros congéneres (no observado en *X. magdalenae*). *Xyliphius sofiae* se diferencia de todos sus congéneres, excepto *X. lepturus,* por la punta del hocico alargado y estrechamente redondeada vs. corto y ampliamente redondeado, a menudo con una pequeña muesca mediana; quinto ceratobranquial relativamente estrecho con los dientes aciculares alargados vs. ampliamente expandidos, en forma de hoja, con dientes cónicos y más amplios; límites anteriores de las aberturas branquiales separadas por la distancia menor que la longitud de la abertura vs. mayor que la longitud de la abertura; los radios de la aleta anal de forma modal nueve vs. siete y la linea lateral extendiendose posteriormente hasta la aleta caudal vs. linea lateral extendiendose posteriormente hasta los hipurales. El único espécimen de *X. sofiae* depositado en colecciones de museos fue colectado en el canal principal del Río Amazonas cerca de Iquitos, Peru y describimos su osteología utilizando técnicas no invasivas: tomografía computarizada en alta resolución. *Xyliphius lombarderoi* Risso and Risso, 1964, especie descrita solamente basado en el holotipo que está perdido, es considerado como sinónimo junior de *X. barbatus* Alonso de Arámburu y Arámburu, 1962. Se resumen características variables de las siete especies de *Xyliphius* tratadas aquí como válidos, y sus distribuciones se representan gráficamente basadas en una extensiva revisión de especímenes en museos.

XYLIPHIUS Eigenmann, 1912 is one of 13 genera of Aspredinidae, a family with about 43 valid species commonly known as banjo catfishes (Friel, 2003; Carvalho et al., 2015; Friel and Carvalho, 2016). Including the new taxon described here, *Xyliphius* contains seven valid species distributed in major watersheds throughout South America, such as the Magdalena, Maracaibo, Orinoco, Amazon, Paraná-Paraguay, and Tocantins (Friel, 2003; Figueiredo and Britto, 2010). In the Western Amazon and Orinoco basins, two species occur together in large tributaries on the Andean piedmont: *Xyliphius lepturus* Orcés, 1962 and *Xyliphius melanopterus* Orcés, 1962. *Xyliphius anachoretes* Figueiredo and Britto, 2010 is known from only two specimens from the upper reaches of the Tocantins basin on the Brazilian Shield and is highly disjunct from congeners. *Xyliphius magdalenae* Eigenman, 1912 and *X. kryptos* Taphhorn and Lilyestrom, 1983 occur west of the Andes as endemics to the Magdalena and Maracaibo basins, respectively. Calviño and Castello (2008) reported on specimens of *Xyliphius barbatus* Alonso de Arámburu and Arámburu, 1962 trawled from depths of 35–45 m in the Middle Paraná River. Specimens of *Xyliphius* are rare in museum collections due to their occurrence in the main channels of medium to large rivers and habitats that require special techniques (e.g., trawling) or conditions (dry downs during dam construction) for effective sampling.

According to Friel (1994), the monophyly of *Xyliphius* is supported by eight unambiguous character state changes: cranium lacking orbital concavity; pterotic laminar process directed laterally and rounded; premaxilla displaced laterally;

[1] Laboratório de Ictiologia, Departamento de Zoologia, Universidade Federal do Rio Grande do Sul, Av. Bento Gonçalves, 9500, 91501-970 Porto Alegre, RS, Brazil; Email: carvalho.ictio@gmail.com. Send reprint requests to this address.
[2] Department of Ichthyology, The Academy of Natural Sciences, 1900 Benjamin Franklin Parkway, Philadelphia, Pennsylvania 19103-1195; Email: (MHS) sabaj@ansp.org.
[3] PUCRS, Faculdade de Biociências, Av. Ipiranga, 6681, 90619-900 Porto Alegre, RS, Brazil; Email: reis@pucrs.br.
Submitted: 20 May 2016. Accepted: 3 October 2016. Associate Editor: W. L. Smith.
 DOI: 10.1643/CI-16-456 Published online: 10 March 2017

suprapreopercle present; lateral end of posterior ceratohyal expanded; bipartite nasal; papillae present on lower jaw; and skin with flattened unculiferous tubercles. Other characteristics not unique to *Xyliphius* but useful for identification include: anterior margin of fleshy tube enclosing anterior nares with finger-like papillae; coronomeckelian bone absent; Meckel's cartilage with high ascending process; and anterior margin of pectoral-fin spine smooth, without serrations (Friel, 1994).

We describe a new species of *Xyliphius* based on a single specimen from the Amazon River channel near Iquitos, Peru. Osteological descriptions are based on high-resolution X-ray computed tomography (HRXCT), a non-invasive technique that reconstructs a virtual skeleton in digital form. High-resolution X-ray computed tomography has been recently used to recover osteological data for species rare in museum collections (Schaefer, 2003; Schaefer and Fernández, 2009; Carvalho and Albert, 2011; Lundberg et al., 2014).

MATERIALS AND METHODS

Measurements were taken point to point with a digital caliper and are expressed as percent of the standard length (SL), except subunits of head, expressed as percent of the head length (HL). Measurements follow Friel (1995) and Cardoso (2010), except for posterior cleithral-process length and head length. Posterior cleithral-process length was taken from the anterior lateral margin of the cleithrum to the posterior tip of process. Head length was taken from snout tip to point along posterior margin of supraoccipital, aside base of supraoccipital process (process visualized beneath thick skin by adpressing caliper tip).

The holotype was scanned at the High-Resolution X-ray Computed Tomography Facility, The University of Texas, Austin, using an NSI scanner with the following settings: high power, 150 kV FeinFocus X-ray source, 0.17 mA, no filter, Perkin Elmer detector, 0.25 pF gain, 2 fps (499.893 ms integration time), no binning, no flip, source to object 133.811 mm, source to detector 1316.553 mm, continuous CT scan, no frames averaged, 0 skip frames, 3000 projections, 7 gain calibrations, 0.762 mm calibration phantom, data range [–50, 600] (grayscale range adjusted from NSI defaults). Voxel size 0.00946 mm. Total slices 1820.

The scan was taken along the long axis of the specimen from snout tip to about the sixth vertebrae. Visualizations and sectioning of the 3D models were produced as 8-bit jpeg files in the software package VGStudio MAX® V1.2.1, at The Academy of Natural Sciences of Drexel University (ANSP). The renderings appear similar to photographs and represent differences in X-ray attenuation based on thickness and density of anatomical structures. The shadowing option in VGStudio was used to enhance 3D visualization. Figures were captured as still frames from HRXCT digital animations and edited for publication in Adobe Photoshop®CS. Cut through videos along the axial, sagittal, and frontal planes and raw images (8-bit jpeg) of X-ray slices were uploaded to Morphobank (www.morphobank.org, project number 2361).

Vertebral counts and descriptions of the caudal region are based on digital radiographs captured at ANSP with a Kevex MicroFocus X-Ray Source and Varian PaxScan image receptor. Vertebral counts include five vertebrae modified into the Weberian apparatus, and the PU1+U1 and U2 elements of the caudal skeleton are counted as a single vertebra. Comparative material was cleared and stained (CS) according to Taylor and Van Dyke (1985). Using Adobe Illustrator®CS and Adobe Photoshop®CS, illustrations were traced and stippled from digital images taken with a Nikon D90 of cleared and stained specimens in 95% glycerin. Whole specimens were digitally imaged with a Nikon D90 using the photo-tank technique described by Sabaj Pérez (2009).

Anatomical descriptions focused on characteristics described in previous phylogenetic studies of the family Aspredinidae (Friel, 1994; de Pinna, 1996; Cardoso, 2008). Anatomical terminology generally follows the Teleost Anatomical Ontology (TAO; Dahdul et al., 2010), an integral part of the Uberon Ontology covering anatomical structures in animals (Mungall et al., 2012; http://uberon.github.io/). GenSeq nomenclature follows Chakrabarty et al. (2013). Genomic DNA was extracted using a DNeasy tissue extraction kit (Qiagen) on muscle and/or fin clips fixed in 96% ethanol and stored at –80°C. Sequences of mitochondrial encoding cytochrome oxidase subunit I (COI) and nuclear encoding myosin, heavy polypeptide 6 (Myh6) and SH3 +PX domain-containing 3-like protein (SH3PX3) were amplified following Herbert et al. (2003) and Li et al. (2007), respectively, and sequenced at Functional Biosciences (Madison, WI). Institutional abbreviations follow Sabaj Pérez (2014).

***Xyliphius sofiae* Sabaj, Carvalho, and Reis, new species**

urn:lsid:zoobank.org:act:AD6D52EE-CF9D-48CA-83FD-4F0C90868920

Figure 1, Tables 1, 2

Xyliphius sp.—Arce et al., 2013:572 [phylogeny outgroup, listed as likely undescribed species].

Holotype.—ANSP 182322, 44.1 mm SL (right pelvic fin taken for tissue), Peru, Loreto, Maynas, Río Amazonas, main channel in vicinity of Iquitos, 03°43′21″S, 073°12′14″W, M. Sabaj, M. Arce, A. Bullard, O. Castillo, C. DoNascimiento, et al., 13 August 2005. GenBank accession numbers (GenSeq-1): KC555831 (rag1; Arce et al., 2013), KC555965 (16S; Arce et al., 2013), KU736764 (COI; this study), KU736765 (Myh6; this study), KU736766 (SH3PX3; this study).

Diagnosis.—*Xyliphius sofiae* is distinguished from congeners by four autapomorphies: eyes absent vs. present (though reduced); color pale, lacking pigment (Fig. 1) vs. head and body darkly pigmented (Fig. 2); branchiostegal rays five vs. four; unculiferous tubercles on posterior body distributed evenly vs. enlarged unculiferous tubercles typically arranged in five distinct rows from above pelvic-fin base to posterior end of caudal peduncle. In addition, the pectoral fin of *X. sofiae* has one ossified proximal radial vs. two in congeners (except *X. magdalenae,* not examined). *Xyliphius sofiae* is distinguished from all congeners except *X. lepturus* by having the snout tip elongated and narrowly rounded (Fig. 3A, C) vs. short and broadly rounded, often with small median notch (Fig. 3B, D); fifth ceratobranchial relatively narrow with two or three irregular rows of acicular teeth vs. broadly expanded with larger conical teeth; anterior limits of the branchial apertures separated by a distance smaller than length of aperture vs. greater than length of aperture; anal-fin rays modally nine vs. seven; and lateral line extending onto base of caudal-fin rays vs. finishing in hypural region.

Description.—Morphometric data summarized in Table 1. Head and body depressed. Dorsal profile rising gently from snout tip to dorsal-fin origin with shallow convexity between

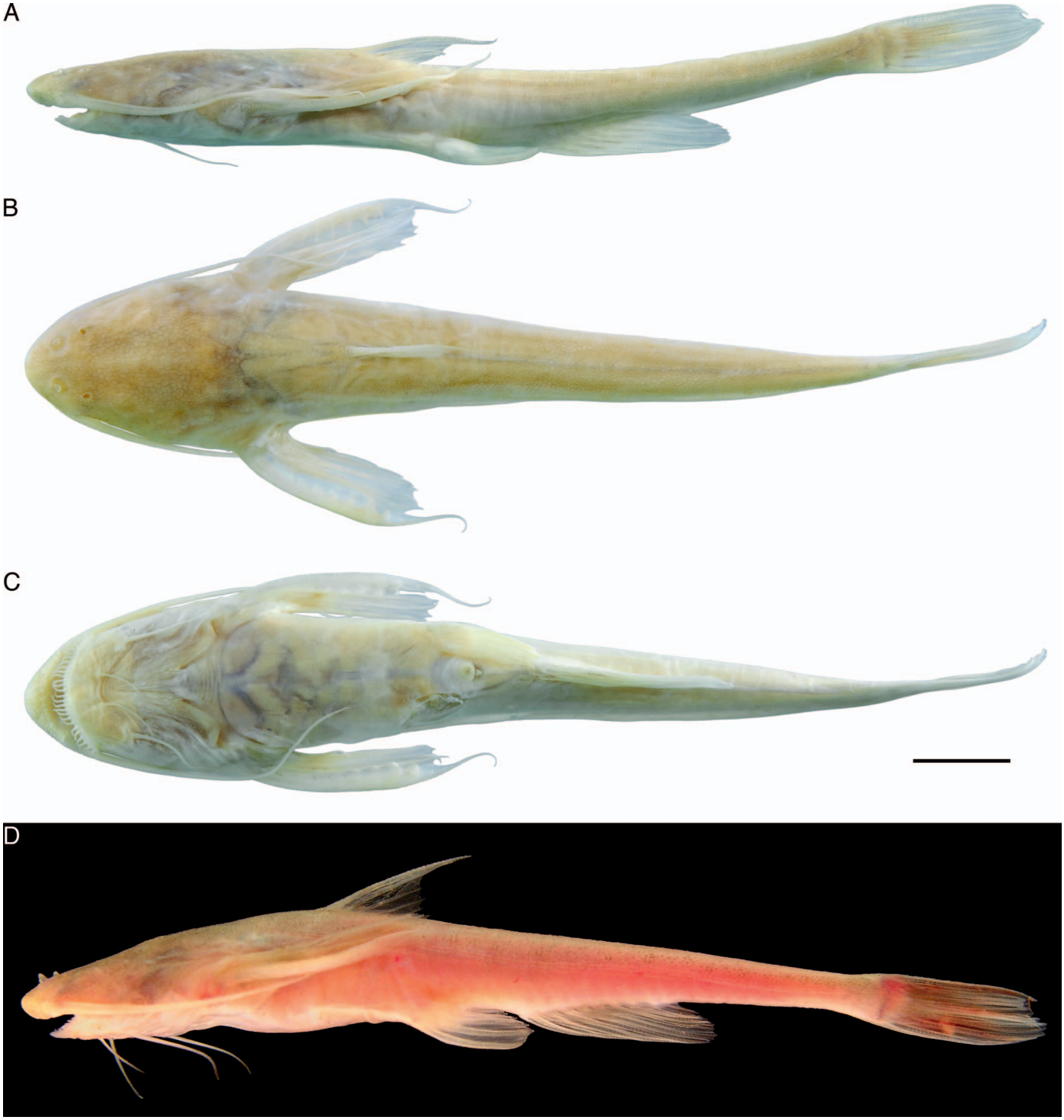

Fig. 1. Holotype of *Xyliphius sofiae*, ANSP 182322, 44.1 mm SL, Río Amazonas in vicinity of Iquitos, Loreto, Peru. (A–C) Alcohol preserved (scale bar = 5 mm). (D) Live. Photos by M. Sabaj.

anterior nares and occipital region; then straight, descending gradually to end of caudal peduncle. Ventral profile more or less flat except for abrupt rise from mouth gape to snout tip. Rostrum bluntly triangular in dorsal view, lacking medial notch. Caudal peduncle long and slender, rounded in cross section.

Eyes absent. Anterior nares located dorsally about midway between snout tip and posterior rictus of mouth, enclosed by fleshy tube with posterior portion enlarged, flap-like; anterior margin of tube with two finger-like papillae projected posteriorly. Posterior nares lacking fleshy tube, aligned with posterior insertion of maxillary barbel. Rostrum overhanging inferior mouth; gape large, spanning distance between lateral contours of snout. Upper lip rugose with small flattened tubercles; lower lip with 31 elongate papillae, all unbranched; length of longest papilla about ten times its width (Fig. 3A).

Three pairs of barbels, all simple. Maxillary barbel long, reaching vertical through base of first branched dorsal-fin ray; leading edge scalloped with low, ridge-like tubercles.

Table 1. Morphometric data for holotype of *Xyliphius sofiae*.

	Measurement (mm)	%
Standard length	44.1	—
Percentages of standard length		
Head length	12.4	28.1
Prepectoral length	12.2	27.6
Cleithral width	9.6	21.7
Maximum head depth at supraoccipital	4.9	11.1
Pectoral-spine length	9.6	21.7
Distance between tips of coracoid processes	7.2	16.3
Posterior coracoid process length	4.1	9.2
Distance between cleithral processes	6.1	13.8
Posterior cleithral-process length	4.3	9.7
Predorsal length	17.1	38.7
Depth at dorsal-spine insertion	4.9	11.1
Dorsal-spine length	7.9	17.9
Prepelvic length	22.1	50.1
Length of 1st pelvic-fin ray	5.9	13.3
Preanal length	27.2	61.6
Anal-fin base length	7.9	17.91
Caudal-peduncle length	10.4	23.5
Caudal-peduncle depth	1.5	3.4
Caudal length	9.6	21.7
Percentages of head length		
Maxillary-barbel length	15.3	123.3
Distance between anterior nares	2.4	19.3
Distance between posterior nares	3	24.1
Mouth width	5.5	44.3

Mental barbels staggered, surfaces slightly rugose. Outer mental barbel long, surpassing posterior margin of scapulocoracoid bridge, and nearly twice as long as inner mental barbel. Opercular opening entirely ventral, concealed by large rounded membranous flap, and nearly reaching its counterpart anteriorly (i.e., anterior limits of opercular openings separated by distance less than length of aperture).

Skin roughened with flattened unculiferous tubercles. Largest tubercles appear as small irregular plates tightly spaced on skin covering neurocranium. Smaller, subtriangular, weakly imbricate tubercles on posterior flanks and not arranged in distinct rows. Smallest tubercles on ventral surfaces. Enlarged and slightly raised tubercles on underside of overhanging snout. Small, oblique, slit-like pore at axilla of pectoral fin. Base of caudal fin covered with skin bearing small triangular tubercles.

Based on HRXCT data, external surfaces of skull-roof bones with pitted texture, lacking bony knobs. Mesethmoid long and deep with cornua weakly projected laterally, elongate anterolateral concavity for articulation with premaxilla (completed by lateral process from ventral face), slight superficial posterolateral expansion for suture with lateral ethmoid, and elongate posterior rami enclosing nearly one-third of anterior cranial fontanel (Figs. 4, 5). Anterior face of mesethmoid with small bony tubercles directed anteroventrally; anterior margin separated by distinct anteromedial notch continuing as dorsal median furrow to midlength (notch not visible in whole specimen). Posterior portion of mesethmoid not elevated, level with anterior portion of frontals. Lateral ethmoid with large internal chamber housing olfactory bulb and large circular foramen on anterolateral face for connection between olfactory bulb and olfactory organ (Fig. 6C, E, F). Lateral ethmoid extended dorsoposteriorly, contributing to small portion of dorsal surface and lateral margin of neurocranium, partially enclosing anterolateral margin of frontal. Lateral ethmoid with large protruding lateral process articulating with central mesial face of autopalatine (Figs. 4A, 5A). Frontal moderately compact with deeply pitted surface; length about three times width; lateral margin lacking orbital concavity; contacting supraoccipital via posteriorly directed arms. Anterior cranial fontanel elongated and narrow, length about 7.5 times width; anterior third enclosed by mesethmoid, remainder by frontals. Posterior cranial fontanel similarly long and narrow, length over nine times width; enclosed mostly by frontals except posteriormost rim formed by supraoccipital. Epiphyseal bar centered along cranial fontanel with broad median suture over one-fifth as long as distance between anterior and posterior limits of fontanel. Supraoccipital compact, greatest length about 1.5 times greatest width; surface smooth anteriorly, pitted posteriorly; posterior process narrow, length nearly three times width, contacting dorsal keel of Weberian complex vertebrae. Sphenotic curved, contacting pterotic, supraoccipital, and posterior half of lateral margin of frontal; surface pitted. Pterotic expanded anteriorly as shelf contacting posterolateral portion of sphenotic; anterolateral margin concave in dorsal view; surface pitted. Pterotic expanded by lateral blade that is somewhat rounded in dorsal view. Supratemporal fossa distinct, enclosed by posterior portions of pterotic and supraoccipital at their suture. Epioccipital compact, contacting supraoccipital anteriorly, pterotic laterally, and posttemporal-supracleithrum posteriorly; dorsal face contributing to skull roof and posteromedial face contributing to posterior wall of cranium. Posttemporal-supracleithrum plate-like with pitted surface, contributing to dorsal aspect of skull; anterolateral process overlying dorsal process of cleithrum.

Premaxilla broad and plate-like with anterior and posterior margins somewhat rounded, surface rugose; teeth absent. Premaxilla lateroventral to mesethmoid and remote from counterpart; dorsolateral margin contacting anterior wing of infraorbital 1. Maxilla long and slender, distally bifurcate for about two-thirds its length with ventrolateral arm longer than dorsomedial one. Dentary slender with symphyseal gap, forming broad arc to accommodate large gape (Fig. 5A). Dentary teeth conical, curved slightly inwards; arranged in two rows, outer row occupying symphyseal half of dentary length, inner row more restricted to symphyseal portion of bone (Fig. 7A). Coronomeckelian bone absent.

Hyomandibula with anterodorsal process contacting ventral face of sphenotic, concave anteroventral face contacting quadrate, and laterally associated with preopercle. Quadrate subtriangular, anterior condyle articulating with retroarticular and anguloarticular, not contacting ventral margin of small metapterygoid (except perhaps by cartilage). Endopterygoid squarish, located beneath and medial to posterior end of autopalatine. Autopalatine moderately compact, length about six times minimum diameter, posterior end truncate, not bifurcate. Opercle boomerang-shaped with posterior wing about twice as long as ventral one. Interopercle present, wedge shaped with dorsoposterior margin firmly attached to ventral wing of opercle (Fig. 7A).

Urohyal present, rounded anteriorly with three posteriorly directed wings and distinct foramen in central portion visible in dorsal view (Fig. 7C). Two ossified basibranchials. First

Table 2. Summary of characteristics variable within valid species of *Xyliphius* based on literature and examined material (Alonso de Arámburu and Arámburu, 1962; Taphorn and Lilyestrom, 1983; Calviño and Castello, 2008; Figueiredo and Britto, 2010). HL = head length, SL = standard length.

Character/species	*X. anachoretes*	*X. barbatus*	*X. kryptos*	*X. lepturus*	*X. magdalenae*	*X. melanopterus*	*X. sofiae*, new species
Snout (% HL)	broadly rounded with medial notch (24.8–28.7)	broadly rounded with medial notch	broadly rounded with medial notch (26.9–33.5)	narrowly rounded, lacking medial notch (32.1–35.3)	broadly rounded (32.4–38.8)	broadly rounded with medial notch (28.1–34.6)	narrowly rounded, lacking medial notch (~40)
Eyes (% HL)	extremely rudimentary (1.5–2.4)	rudimentary	rudimentary (2.3–3.9)	rudimentary (2.0–4.0)	small (4.2–4.7)	rudimentary (2.9–3.9)	anophthalmic
Maxillary barbel (% SL)	short (16.8–19.2)	not measured	moderate (21.6–29.2)	moderate (24.0–28.3)	short (17.8–18.9)	moderate (20.7–25.1)	long (34.7)
Lower lip papillae	22–24 simple or with few minute ventral branches	28–30 with many ventral branches arranged as arborescence	22–29 simple or with few minute ventral branches	24–28 with many ventral branches arranged as arborescence	21–22 simple or with few minute ventral branches	24–26 with many ventral branches arranged linearly	30 simple
Cleithral width (% SL)	wide (25.6–30)	wide (27.0–28.4)	wide (25.8–27.7)	narrow (22.0–26.7)	narrow (23.9–26.4)	wide (24.3–27.7)	narrow (21.7)
Anal-fin rays	7	6–8 (modally 7)	7–8 (modally 7)	8–10 (modally 9)	6–7 (modally 7)	7–8 (modally 7)	9
Maximum SL (mm)	88.4	125	130	132	80	147	44.1
Total vertebrae	36 (n = 1 spec.)	36 (n = 1 spec.)	38–39, n = 38 (n = 3 spec.; mode 38)	36–39, modally 39 (n = 5 spec.; mode 39)	40 (n = 1 spec.)	37–38, modally 37 (n = 5 spec.; mode 37)	36 (n = 1 spec.)
Caudal-peduncle depth (% SL)	deep (8.0–8.3)	moderate (6.6–7.5)	deep (8.4–9.1)	shallow (4.5–5.2)	deep (7.9–8.2)	moderate (6.5–7.5)	very shallow (3.4)
Posterior terminus of lateral line end	in hypural region	in hypural region	in hypural region	on base of caudal-fin rays	in hypural region	in hypural region	on base of caudal-fin rays
Teeth on 5th ceratobranchial tooth plate	conical, supported by expanded plate	conical, supported by expanded plate	conical, supported by expanded plate	acicular, limited to slender ceratobranchial	conical, supported by expanded plate	conical, supported by expanded plate	acicular, limited to slender ceratobranchial
Orientation of 5th parapophyses	deflected anteriorly	deflected anteriorly	lateral	lateral	lateral	deflected anteriorly	lateral
Gas-bladder encapsulation	partial	partial	free	free/partial	free	partial	partial
Rows of tubercles on posterior body	5 longitudinal	5 longitudinal	5 longitudinal	1 middorsal + 5 longitudinal	5 longitudinal	5 longitudinal	lacking

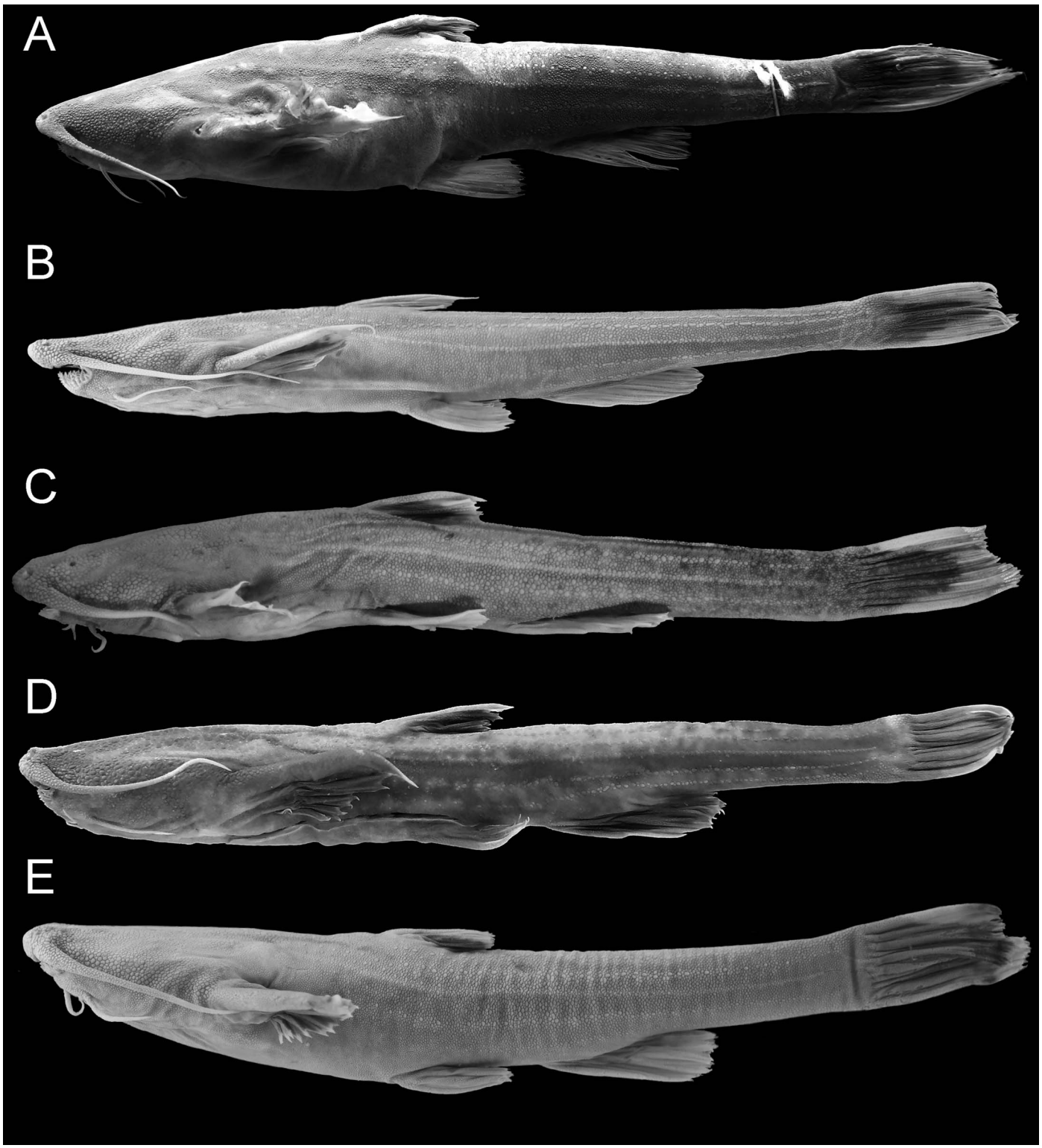

Fig. 2. Lateral view of select species of *Xyliphius*. (A) *X. barbatus*, MLP 6798, holotype, 92.0 mm SL. (B) *X. lepturus*, ANSP 128941, 94.5 mm SL. (C) *X. magdalenae*, CZUT-IC 1288, 75 mm SL. (D) *X. melanopterus*, FMNH 99495, 120.4 mm SL. (E) *X. kryptos*, MCNG 27310, 112.0 mm SL. Photos by M. Sabaj (A), T. Carvalho (B, E), J. Garcia-Melo (C), and A. Thomaz (D).

hypobranchial ossified. Dorsal hypohyal absent. Ventral hypohyal triangular. Anterior ceratohyal broad with expanded lamina along anterolateral margin, contacting posterior ceratohyal via interdigitated suture. Interhyal present, compact, squarish, located anterodorsal to posterior portion of posterior ceratohyal. Branchiostegal rays five; outermost (fifth) with anterior half expanded, approximating size of posterior ceratohyal; fourth branchiostegal ray also with expanded basal portion; remaining branchiostegals 3–5 becoming gradually shorter and more slender, ray-like. Five ceratobranchials, all bearing short gill rakers; fifth ceratobranchial with two or three irregular rows of acicular teeth along dorsal surface of anterior half (Fig. 8B). Four epibranchials, third bearing distinct uncinate process (Fig. 8). First

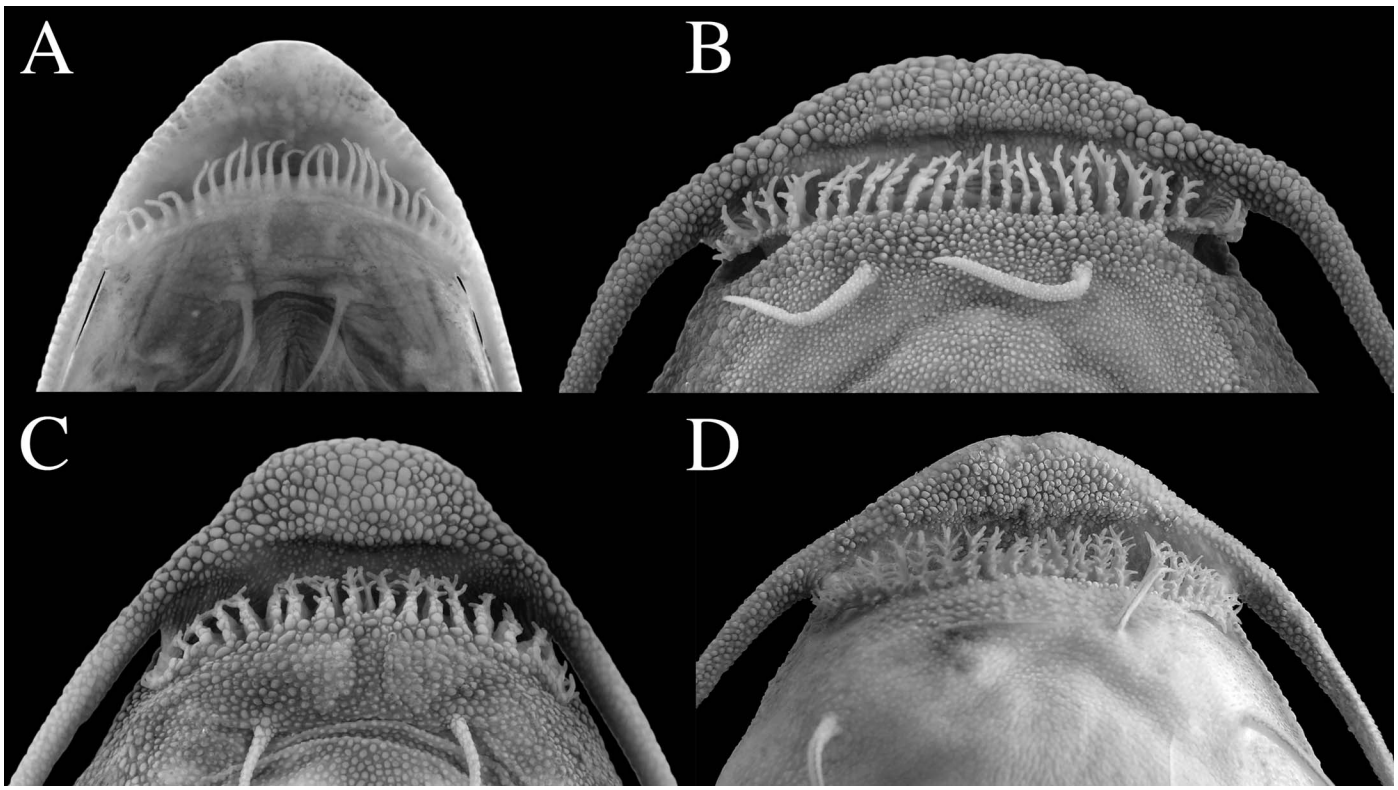

Fig. 3. Ventral view of head. (A) *Xyliphius sofiae*, ANSP 182322, holotype, 44.1 mm SL. (B) *X. melanopterus*, FMNH 99495, 120.4 mm SL. (C) *X. lepturus*, ANSP 128941, 94.5 mm SL. (D) *X. barbatus*, MLP 6798, 92.0 mm SL. Photos by M. Sabaj.

and second pharyngobranchials absent or unossified; third and fourth ossified, suspending expanded tooth plate with elongate acicular teeth.

Nasal composed of two separate tubular ossifications between supraorbital sensory pores 1–2 and 2–3, respectively (Fig. 6A). Infraorbital 1 with anterior half curved medially, finishing dorsal to premaxilla (Fig. 4A); mesial limb short; lateral face notched with foramen for canal passage posteriorly (Fig. 6A, D). Remaining infraorbitals reduced to series of small, disjointed tubules, some with small ventrolateral ossification associated with branch for infraorbital canal pores i4–i6. Additional small canal-like ossifications situated between pores i1–i2, ventrolateral to infraorbital sensory branch 2, and dorsomedial to infraorbital 1. Infraorbital canal (Fig. 6A) begins with pore (i1) and enters foramen at midpoint of dorsal margin of infraorbital 1; second pore (i2) at end of branch posteromedial to pore 1. Infraorbital canal exits through foramen in posterior notch in infraorbital 1 and begets four branches ending in pores i3–i6. Preopercle-mandibular canal (Fig. 7) incomplete anteriorly with one short tubular ossification ventral to posterior portion of dentary, separated by gap from second similar ossification beneath posterior portion of retroarticular. Second ossification separated by gap from disjointed series of closely set ossified tubules finishing with canal passage into preopercle. Preopercle-mandibular canal associated with hyomandibula posteriorly. Suprapreopercle present, small, bearing canal, received by notch in hyomandibula anteriorly and contacting pterotic posteriorly. Extrascapula present, small tubular ossification located between pterotic and posttemporal-supracleithum (Fig. 4A, B) and at ramification of postotic sensory branch 2. Lateral line complete, not associated with fourth parapophysis, exiting posterolateral corner of post-temporal-supracleithum and extending onto base of caudal-fin rays as simple ossified tubes.

Dorsal keel of Weberian complex with straight margin reaching surface of body. Parapophysis of fourth vertebra forming broad lamina partially encapsulating gas bladder (Fig. 9C). Posterior margin of parapophysis of fourth vertebra in complete contact with ventrally displaced parapophysis of fifth vertebrae. Parapophysis of fifth vertebra long, extending to body wall and beyond lateral limits of parapophysis of fourth vertebra. Distal margin of fifth parapophysis obliquely truncate, not distinctly expanded. No evidence of separate anterior nuchal plate. Middle nuchal plate small, posterolaterally contacting posterior nuchal plate, distant from dorsal keel of Weberian complex. Posterior nuchal plate with acute triangular wing directed anterolaterally (visible in whole specimen). Total vertebrae 36. Vertebrae 7–27 bearing horizontal transverse processes. Hemal and neural spines moderately elongate, those on posterior portion of caudal peduncle obliquely orientated. Seven pairs of ribs on vertebrae 6–12.

Dorsal fin I,4. First ray simple, slender, stiffened (not pungent), and elongated distally as flexible filament; anterior face lacking serrations, but rugose with small plate-like tubercles resembling those on body. Soft rays unbranched, distal tip surpassing intervening membrane. Last dorsal-fin ray not adnate to dorsum by membrane. Pectoral fin I,5. Rigid pectoral spine extended by thin, flexible filament. Anterior face of pectoral-fin spine lacking serrations, but rugose with flat, imbricate tubercles with irregular posterior margin (those on distal filament resemble minute serrations). Posterior face of pectoral-fin spine with eight retrorse dentations; most proximal one small and inconspicuous, remaining ones increasing gradually in size; length of largest dentations approximating width of spine shaft. Soft pectoral-

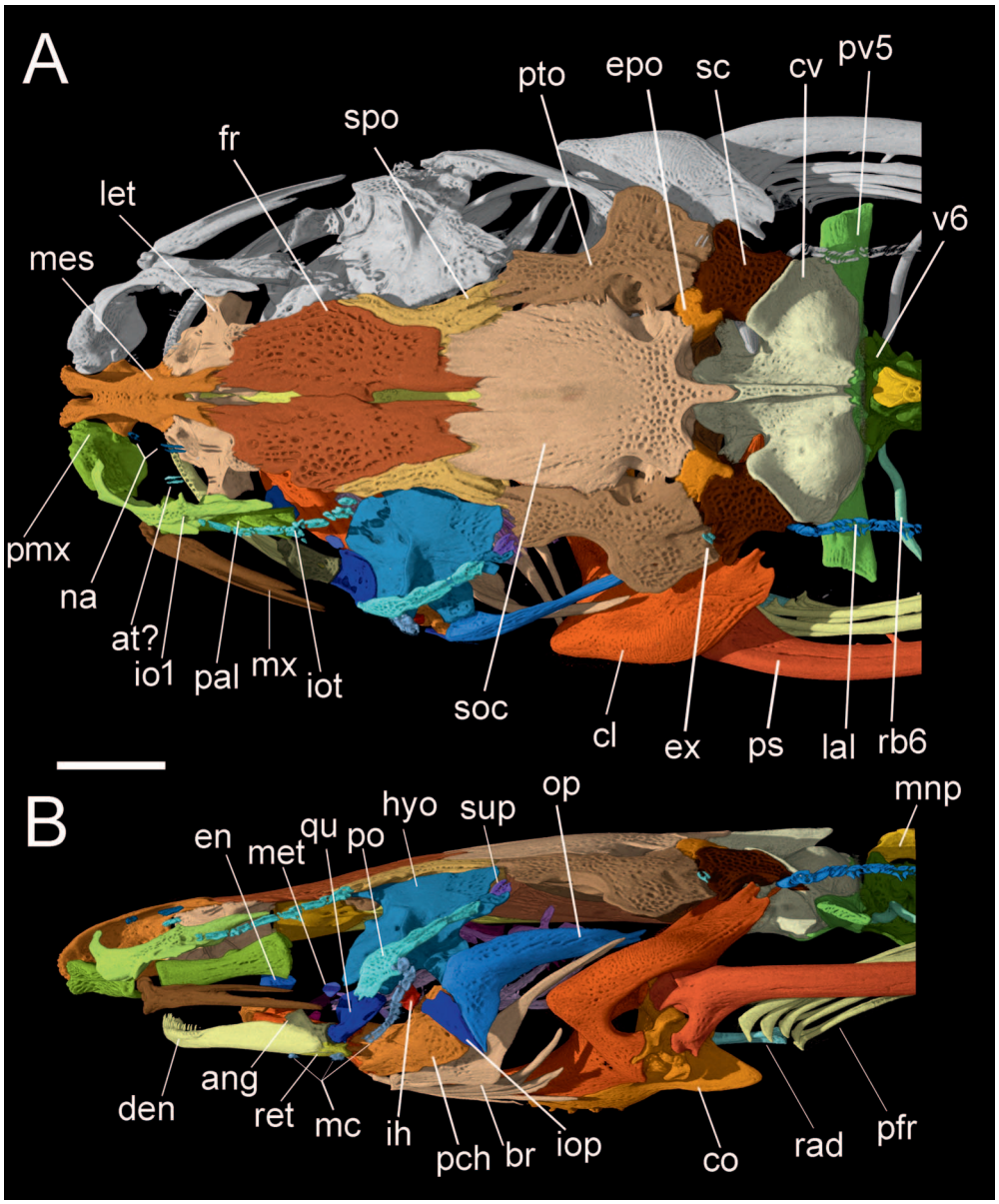

Fig. 4. HRXCT model of skull and anterior body of *Xyliphius sofiae*, ANSP 182322, holotype, 44.1 mm SL. (A) Dorsal view. (B) Lateral view of left side. ang: anguloarticular; at: antorbital tubule; br: branchiostegal rays; cl: cleithrum; co: scapulocoracoid; cv: complex vertebrae; den: dentary; en: endopterygoid; epo: epioccipital; ex: extrascapular; fr: frontal; hyo: hyomandibula; ih: interhyal; io1: infraorbital 1; iop: interopercle; iot: infraorbital tubules; lal: lateral line tubules; let: lateral ethmoid; mc: mandibular canal tubules; mes: mesethmoid; met: metapterygoid; mnp: middle nuchal plate; mx: maxilla; na: nasal; op: opercle; pal: autopalatine; pch: posterior ceratohyal; pfr: pectoral-fin rays; pmx: premaxilla; po: preopercle; ps: pectoral-fin spine; pto: pterotic; pv5: parapophysis of vertebra five; qu: quadrate; rad: pectoral-fin radial; rb6: rib six; ret: retroarticular; sc: posttemporal-supracleithrum; soc: supraoccipital; spo: sphenotic; sup: suprapreopercle; v6: vertebrae six. Scale bar = 2 mm.

fin rays branched except for last one; distal tip of ray surpassing intervening membrane. Single ossified proximal radial associated with pectoral-fin rays two and three. Dorsal wing of cleithrum with three processes: dorsal process long and narrow with posteriorly directed keel; middle process short, truncated; ventral process (posterior cleithral process) scarcely evident as distal extension of obliquely oriented cleithral bulge (portion receiving dorsal process of pectoral spine). Ventral blade of pectoral girdle with single foramen laterally displaced and posterior to contact of cleithrum and scapulocoracoid. Posterior process of scapulocoracoid slender and moderately elongate, extending posterolaterally to vertical through tip of posterior cleithral process. Pelvic fin i,6; second and third rays longest, just reaching anal-fin origin. Lateral arm of basipterygium well developed anteriorly, reaching vertical through eighth vertebrae. Anal fin iv,5. Caudal fin with ten principal rays, five in each lobe; distal margin obliquely truncate with lower lobe slightly longer than upper. Outermost principal caudal-fin rays unbranched; proximal portion expanded and covered with small, flat, imbricate tubercles. Procurrent caudal-fin rays small and difficult to visualize via radiographs, likely two dorsal procurrent rays and three ventral. Adipose fin absent.

Coloration.—Alcohol-preserved specimen pale tan to white (Fig. 1). Fins hyaline except for diffuse melanophores associated with proximal portion of anal-fin rays and extremely faint dusky blotch on basal half of middle caudal fin. Live specimen tan with salmon pink flanks (Fig. 1).

Distribution and habitat.—*Xyliphius sofiae* is known from a single locality in the Amazon River near the town of Iquitos, Peru (Fig. 10). The specimen was collected using a large floating net stretched between two canoes and dragged downstream through the water column.

Etymology.—In honor of the daughter of first author on the specific epithet, for inspiring wisdom in her father.

DISCUSSION

Xyliphius sofiae has the eight features proposed by Friel (1994) as synapomorphies for the genus: cranium lacking orbital concavity (Fig. 4); pterotic laminar process directed

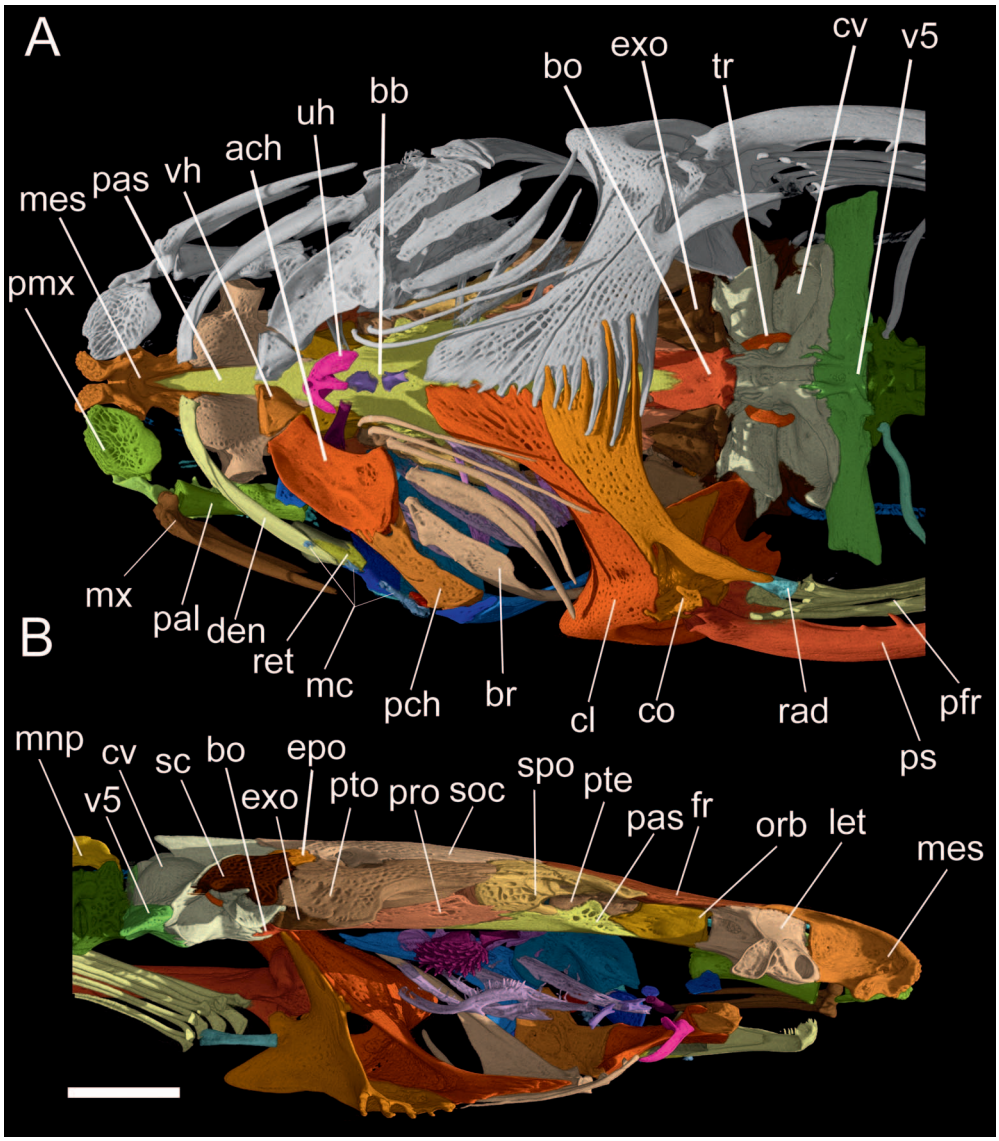

Fig. 5. HRXCT model of skull and anterior body of *Xyliphius sofiae*, ANSP 182322, holotype, 44.1 mm SL. (A) Ventral view. (B) Mesial view of left side. ach: anterior ceratohyal; bb: basibranchials; bo: basioccipital; br: branchiostegal rays; cl: cleithrum; co: scapulocoracoid; cv: complex vertebrae; den: dentary; epo: epioccipital; exo: exoccipital; fr: frontal; let: lateral ethmoid; mc: mandibular canal tubules; mes: mesethmoid; mnp: middle nuchal plate; mx: maxilla; orb: orbitosphenoid; pal: autopalatine; pas: parasphenoid; pch: posterior ceratohyal; pfr: pectoral-fin rays; pmx: premaxilla; pro: prootic; ps: pectoral-fin spine; pte: pterosphenoid; pto: pterotic; rad: pectoral-fin radial; ret: retroarticular; sc: posttemporal-supracleithrum; soc: supraoccipital; spo: sphenotic; tr: tripus; uh: urohyal; v5: vertebrae five; vh: ventral hypohyal. Scale bar = 2 mm.

laterally and rounded (Fig. 4); premaxilla displaced laterally (Fig. 5); suprapreopercle present (Fig. 7A); lateral end of posterior ceratohyal expanded (Fig. 7B-C); bipartite nasal (Fig. 6A); papillae present on lower jaw (Fig. 3A); and skin with flattened unculiferous tubercles (Fig. 2). An additional feature reported here, and newly discovered for Aspredinidae, is lateral ethmoid with enlarged internal chamber housing olfactory bulb (Fig. 6E, F). Computed tomography uncovered this internal structure that is likely a synapomorphy for *Xyliphius*. We observed a similar rounded bulge (e.g., Fig. 6B) on the ventral surface of the lateral ethmoid in cleared and stained specimens of *X. lepturus*, *X. kryptos*, and *X. melanopterus*. The bony bulge suggests that the lateral ethmoid is hollowed by an enlarged rounded internal chamber, as in *X. sofiae*.

Xyliphius sofiae shares features with *X. lepturus* that are variably supportive of a sister-group relationship: snout relatively elongate and narrowly rounded, lacking median notch (Fig. 3A, C); fifth ceratobranchial narrow with two or three irregular rows of acicular teeth (Fig. 8A–C); anterior limits of branchial apertures separated by distance less than length of aperture (Fig. 1); anal-fin rays modally nine; and lateral line extending onto base of caudal-fin rays. The anterior snout margin is truncate in most aspredinids (e.g., *Bunocephalus*, *Pseudobunocephalus*, and Aspredininae) and may include a small median notch in groups such as *Pterobunocephalus* and Hoplomyzontinae. Anal-fin ray counts are difficult to polarize in Aspredinidae because they range widely from six in *Acanthobunocephalus*, *Amaralia, Dupouyichthys*, and some species of *Hoplomyzon* to more than 50 in Aspredininae (Mees, 1987). The modal number of anal-fin rays in *X. lepturus* and *X. sofiae* is nine compared to seven in remaining congeners. A broad and leaf-shaped fifth ceratobranchial bearing several rows of enlarged teeth (Fig. 8D) is a potential synapomorphy for all species of *Xyliphius* except *X. lepturus* and *X. sofiae*. In most aspredinids, the fifth ceratobranchial is relatively slender and elongate, as in *X. lepturus* and *X. sofiae*, but varies in terms of tooth distribution. The teeth may be widespread along the dorsal portion of the bone (Fig. 8B, C), as in *X. sofiae*, or limited to its mesial portion, as in all remaining aspredinids except *Aspredo*, *Aspredinichthys*, and *Platystacus* (Friel, 1994:ch. 49). Two features are unique to *X. lepturus* and *X. sofiae* within Aspredinidae and most strongly support their relationship as sister taxa. *Xyliphius lepturus* and *X. sofiae* are the only aspredinids that have a lateral line extending posteriorly onto base of caudal-fin rays, a condition sometimes observed in Auchenipteridae. *Xyliphius lepturus* and *X. sofiae* also share

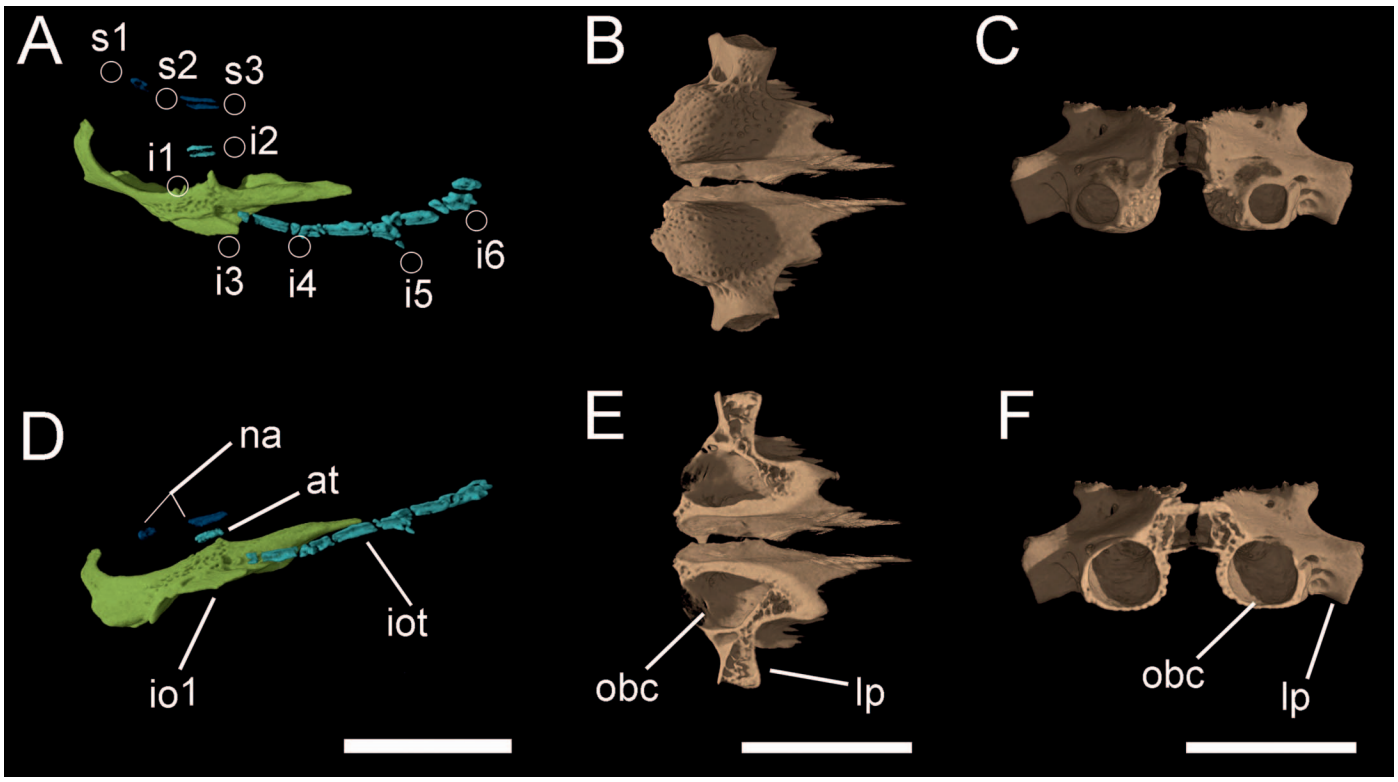

Fig. 6. HRXCT model of select bones in *Xyliphius sofiae*, ANSP 182322, holotype, 44.1 mm SL. Bones associated with the anterior cephalic canals of the lateral line system (anterior is left) in dorsal (A) and lateral (B) views. Entire lateral ethmoid (anterior is left) in ventral (C) and frontal (D) view. (E) Partial lateral ethmoid in dorsal view cut to about half of its depth (anterior is left). (F) Partial lateral ethmoid in frontal view cut to about vertical through origin of lateral process. at: antorbital tubule; i1–i6: infraorbital branches one to six; io1: infraorbital one; iot: infraorbital tubules; lp: lateral process of lateral ethmoid; na: nasal; obc: olfactory bulb chamber; s1–s3: supraorbital branches one to three. Scale bar = 2 mm.

a long branchial aperture obliquely extended towards isthmus (anterior limits separated by distance less than length of aperture). The remaining aspredinids have relatively short branchial apertures with anterior limits separated by distance greater than length of aperture (Friel, 1994:ch. 31).

In Aspredinidae, the gas bladder lies beneath the lateral wings of the parapophyses of the fourth vertebrae, which is incorporated into the Weberian complex. In all aspredinid genera as well as *X. magdalenae* and *X. kryptos,* the gas bladder is not encapsulated by bone (Fig. 9A). In *Xyliphius sofiae*, *X. anachoretes*, *X. barbatus*, and *X. melanopterus*, the fourth parapophyses partially enclose the gas bladder posteroventrally (Fig. 9B, C). Most cleared and stained specimens of *X. lepturus* exhibit no ventral encapsulation; however, the gas bladder was partially encapsulated ventrally in one specimen (MCNG 5547) from the Apure River (Orinoco Basin). Polymorphism in *X. lepturus* aside, gas bladder encapsulation in *X. sofiae* is unique and differs from that observed in *X. anachoretes*, *X. barbatus*, and *X. melanopterus*. In *X. sofiae*, only a small portion of the fourth parapophyses posteroventrally encapsulates the gas bladder. In *X. anachoretes*, *X. barbatus*, and *X. melanopterus,* a comparatively large portion of the gas bladder is cradled posteroventrally by a pocket of laminar bone. The difference may reflect two independent evolutionary events for gas bladder encapsulation in *Xyliphius*. In addition, *X. anachoretes*, *X. barbatus*, and *X. melanopterus* share a relatively long and narrow fourth parapophysis (length about one time its width) and fifth parapophysis deflected anteriorly (Fig. 9B), conditions suggestive of a close relationship. In the remaining species of *Xyliphius*, the fourth parapophysis is shorter and broader (length closer to half its width) and the fifth parapophysis is directed laterally (Fig. 9A), conditions that are putatively plesiomorphic within *Xyliphius*.

A peculiar feature shared by all species of *Xyliphius* is a row of 21–30 elongate papillae along the entire lower lip margin that project anteriorly towards the upper lip (Fig. 3; Alonso de Arámburu and Arámburu, 1962; Figueiredo and Britto, 2010:fig. 2). The papillae presumably help sense food items in stygian habitats and exhibit both interspecific and ontogenetic variation. In *X. sofiae*, the labial papillae are all simple, without branches (Fig. 3A). In *X. kryptos* (Maracaibo Basin), *X. magdalenae* (Magdalena Basin), and *X. anachoretes* (Tocantins Basin), each papilla has a few minute branches along its ventral margin. In contrast, *X. melanopterus* (Amazon and Orinoco basins; Fig. 3B) has well-developed ventral branches (contra Figueiredo and Britto, 2010) arranged in linear fashion with successive branches pointing in opposite directions. In *X. lepturus* (Amazon and Orinoco basins; Fig. 3C) and *X. barbatus* (Paraná Basin; Fig. 3D), the ventral branches similarly diverge in opposite directions but are more numerous and impart an arborescence to each labial papilla. Ontogenetically, the ventral branches of the labial papillae vary in number and degree of development (as suggested by Figueiredo and Britto, 2010). The ventral branches are typically smaller and more aligned in juveniles and become larger and oriented in opposite directions in adults. For example, the lower labial papillae are simple and unbranched in the smallest specimen examined of *X. lepturus* (17.8 mm SL; FMNH 99486) and become arborescent with highly developed branches in adults. Such observations

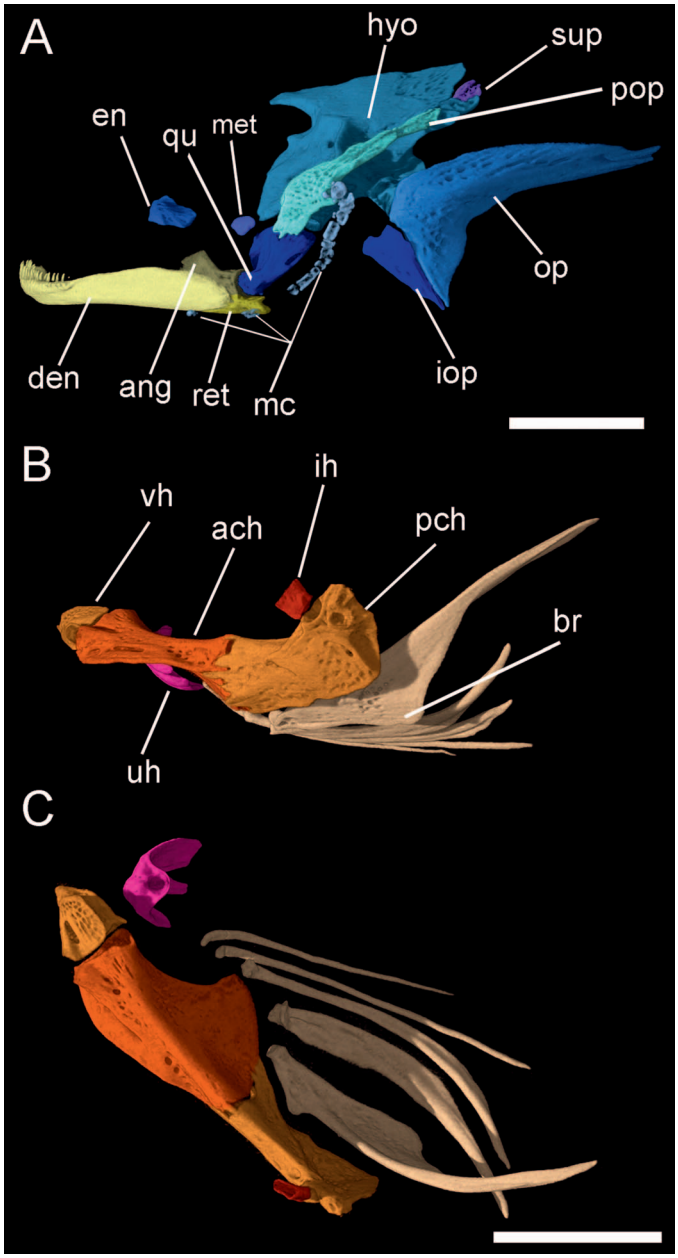

Fig. 7. HRXCT model of suspensorium plus lower jaw (A) and hyoid arch (B–C) of *Xyliphius sofiae*, ANSP 182322, 44.1 mm SL. ach: anterior ceratohyal; ang: anguloarticular; br: branchiostegal rays; den: dentary; en: endopterygoid; hyo: hyomandibula; ih: interhyal; iop: interopercle; mc: mandibular canal tubules; met: metapterygoid; op: opercle; pch: posterior ceratohyal; pop: preopercle; qu: quadrate; ret: retroarticular; sup: supra-preopercle; uh: urohyal; vh: ventral hypohyal. Scale bar = 2 mm.

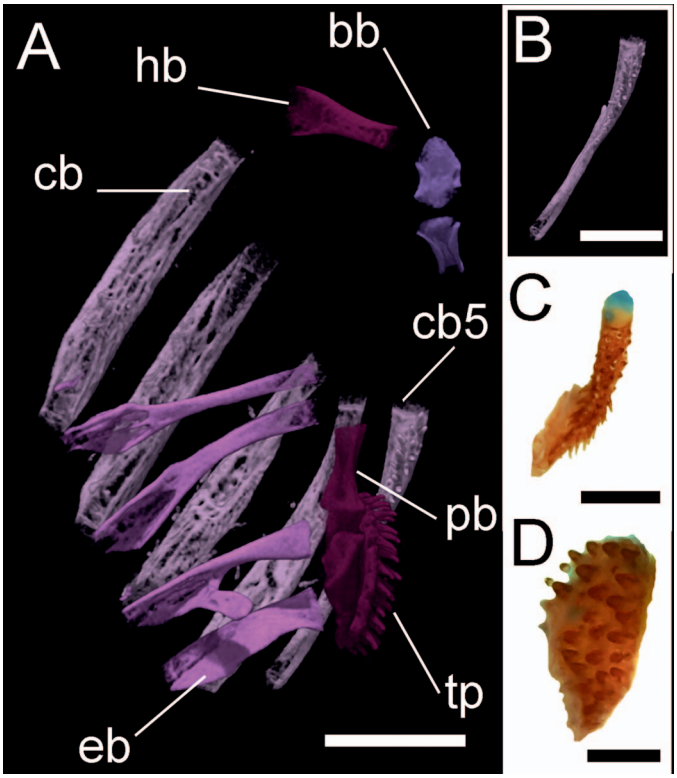

Fig. 8. HRXCT model of branchial arches (A–B, left side, dorsal view, anterior up), and 5th ceratobranchial of cleared and stained specimens (left side, dorsal view, anterior up). (A) *Xyliphius sofiae*, ANSP 182322, holotype, 44.1 mm SL (scale bar = 2 mm). (B) Unobscured dorsal view of 5th ceratobranchial in ANSP 182322 (scale bar = 1 mm). (C) *Xyliphius lepturus*, FMNH 99488, 72.1 mm SL (scale bar = 1 mm). (D) *Xyliphius melanopterus*, FMNH 99493, 81.9 mm SL (scale bar = 1 mm). bb: basibranchial; cb: ceratobranchial; cb5: ceratobranchial five; eb: epibranchial; hb: hypobranchial; pb: pharyngobranchial; tp: tooth patch.

suggest that simple labial papillae in *X. sofiae* represent a pedomorphic condition.

Species of *Xyliphius* are commonly found in the main channel of large whitewater rivers (Fig. 10). Based on museum records, the distributions of four species are largely restricted to the upland portions of large rivers on the Andean piedmont. Two species, *X. lepturus* and *X. melanopterus,* are sympatric in tributaries of the Amazon and Orinoco rivers. *Xyliphius sofiae* uniquely occurs in a relatively lowland stretch (ca. 84 m above sea level) of the upper Amazon.

Xyliphius occupy in deepwater habitats based on their appearance in trawls. Calviño and Castello (2008) collected *X. barbatus* at depths of 35–45 m using trawl nets in the Paraná River. The difficulty of sampling deepwater habitats in large river channels most likely explains the rarity of specimens in museum collections and perhaps the absence of records from lowland whitewater rivers. That said, the extensive trawling surveys of the Calhamazon Project did not record *Xyliphius* from the main channel of the Brazilian Solimões-Amazon and the lower reaches of its major tributaries. Though rare in museums, *Xyliphius* is probably not rare in its preferred habitat. For example, a total of 54 specimens of *X. lepturus* (MCNG 5547, 5549) and one *X. melanopterus* (MCNG 5548) were collected in two days from the dried down riverbed of the Boconó River below the Peña Larga dam after its spillways were closed to fill the Tucupido Reservoir (D. Taphorn, pers. comm., 2016). Some species of *Xyliphius*, including *X. sofiae*, are occasionally caught by ornamental fishermen and sold as aquarium fishes.

Within *Xyliphius, X. sofiae* is best adapted for the darkest depths of large, sediment-rich river channels. Although reduction in eye size is typical of congeners (Table 2), only *X. sofiae* exhibits no external evidence of eyes. Unlike its congeners, *X. sofiae* is extremely pale, almost completely lacking in pigmentation. Additional characteristics such as long barbels and dorsal and pectoral spines extended by flexible filaments may represent tactile adaptations for murky depths. Furthermore, *X. sofiae* is presumably the smallest species of *Xyliphius*. Reduction in eyes, pigmentation, and adult body size are traits commonly found among

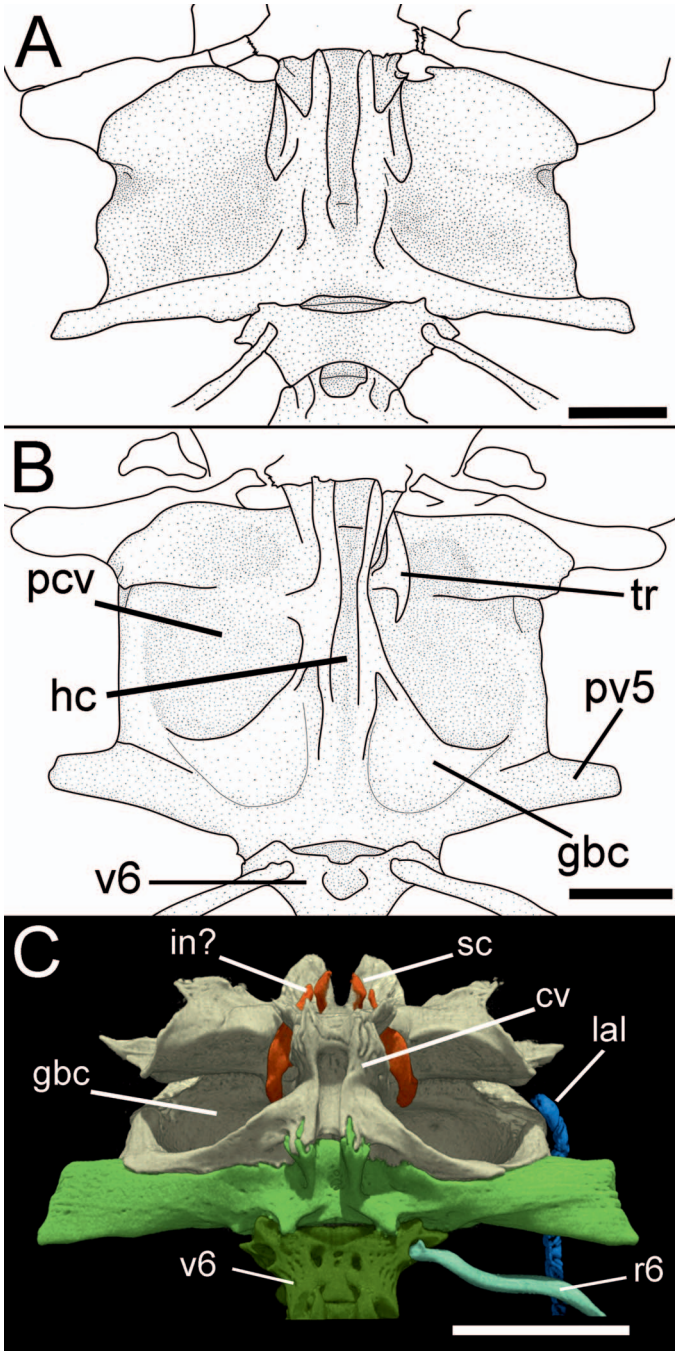

Fig. 9. Ventral view of Weberian complex in select species of *Xyliphius* (anterior is top). (A) *X. lepturus*, FMNH 99488, 72.1 mm SL. (B) *X. melanopterus*, FMNH 99493, 81.9 mm SL. (C) *Xyliphius sofiae*, ANSP 182322, 44.1 mm SL. cv: complex vertebra; gbc: gas bladder chamber (line points to portion encapsulated by bone in B); hc: hemal canal; in: intercalarium; lal: lateral line tubules; pcv: parapophysis complex vertebra; pv5: parapophysis vertebra five; r6: rib 6; sc: scaphium; tr: tripus; v6: vertebra six. Scale bar = 2 mm.

Neotropical fishes inhabiting the deep channels of white-water rivers (Stewart et al., 2002). Within Aspredinidae, eye loss, pale coloration, and small body size have evolved independently in the subfamily Hoplomyzontinae, specifically *Micromyzon akamai* and a putatively related species from the Orinoco River (Friel and Lundberg, 1996). The same three traits help diagnose *Cetopsis oliveirai* (Lundberg and Rapp Py-Daniel, 1994), a cetopsid catfish collected syntopically with *X. sofiae* (MHS, pers. obs.) that also exhibits elongate dorsal-

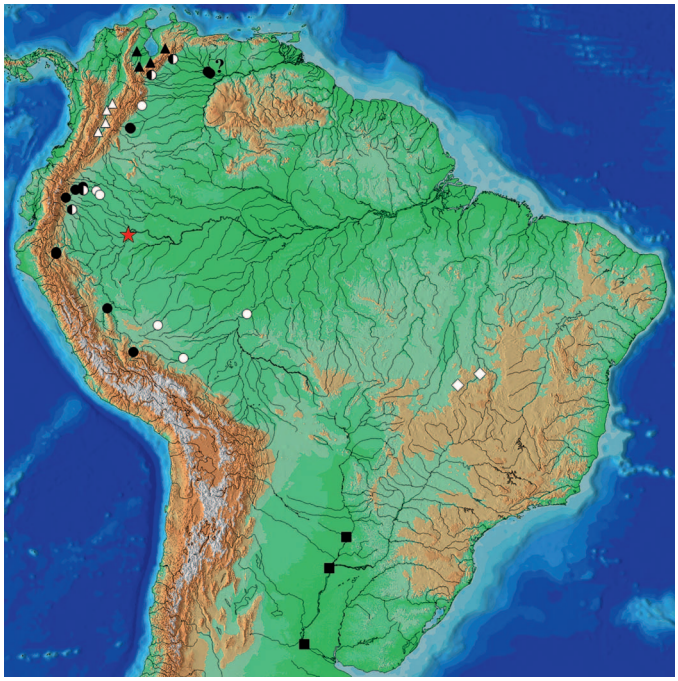

Fig. 10. Distributions of valid species of *Xyliphius* based on museum specimens and literature accounts (Alonso de Arámburu and Arámburu, 1962; Orcés, 1962; Taphorn and Marrero, 1993; Maldonado-Ocampo et al., 2005; Figueiredo and Britto, 2010; Ohara and Zuanon, 2013). Black triangles = *X. kryptos*; white triangles = *X. magdalenae*; white circles = *X. melanopterus*; black circles = *X. lepturus*; star = *X. sofiae*; black squares = *X. barbatus*; white diamonds = *X. anachoretes*; circles half black, half white mark localities where *X. melanopterus* and *X. lepturus* were collected together.

and pectoral-fin ray filaments. Reduced eyes and pale coloration are also found in apteronotid knifefishes (Hilton et al., 2007; Ivanyisky and Albert, 2014) and loricariid catfishes such as *Loricaria pumila,* the smallest species of that genus (Thomas and Rapp Py-Daniel, 2008). In sum, a variety of morphological adaptations place *X. sofiae* at the end of an adaptive continuum for stygian habitats.

***Comments on* Xyliphius lombarderoi.**—Risso and Risso (1964) described *X. lombarderoi* based on a unique holotype (now lost) collected in the Río Paraná just below the mouth of the Río Paraguay. They compared their new species to the nominal *X. lepturus* and *X. melanopterus*, and noted distinguishing similarities with the latter (e.g., snout tip with medial notch, caudal peduncle relatively deep). The authors also compared *X. lombarderoi* to "X. labrosus", a *nomen nudum* clearly referable to the nominal *X. barbatus* described by Alonso de Arámburu and Arámburu (1962) based on two specimens from the lower Paraná, nearly 700 river kilometers downstream from the type locality of *X. lombarderoi* (Friel, 2003).

Risso and Risso (1964) distinguished *X. lombarderoi* based on meristic and morphological characteristics differing from those in the original description of *X. barbatus* (Alonso de Arámburu and Arámburu, 1962). Meristic differences included labial papillae 28 in *X. lombarderoi* (vs. 30 in *X. barbatus*); pectoral fin I,4 (vs. I,5); anal-fin rays 6 (vs. 7), and pectoral spine with 8 (vs. 7) posterior denticulations. Risso and Risso (1964) also distinguished *X. lombarderoi* from *X. barbatus* by having much shorter mandibular barbels, ventral profile rising 20° from pelvic-fin origin to snout, more pronounced

predorsal protuberances, posterior portion of head with two pairs of dorsal ridges converging posteriorly (no lateral ridge), and different coloration. Most of the features used to distinguish *X. lombarderoi* fall within the range of variation observed for *X. barbatus* (Calviño and Castello, 2008; Material Examined herein). Exceptions are the counts reported by Risso and Risso (1964) for the pectoral fin (I,4) and anal fin (6 rays), both of which represent low extremes for *Xyliphius*. Based on specimens examined here and counts reported by Alonso de Arámburu and Arámburu (1962) and Calviño and Castello (2008), *X. barbatus* has pectoral fin I,5 and anal-fin rays 7–8 (modally 7). Risso and Risso (1964) may have mistakenly counted fin-rays for *X. lombarderoi*, or the range of variation known for *X. barbatus* is based on too few specimens. Aside from Risso and Risso's (1964) account, there is no further evidence for two species of *Xyliphius* occurring in the Paraná basin. Therefore, we treat *Xyliphius lombarderoi* Risso and Risso, 1964 as a subjective junior synonym of *Xyliphius barbatus* Alonso de Arámburu and Arámburu, 1962.

MATERIAL EXAMINED

Type specimens lost or not examined firsthand denoted by asterisk.

Xyliphius anachoretes Figueiredo and Britto, 2010: Brazil: Goiás: MNRJ 31923, holotype, 88.4 mm SL, rio Tocantins in marginal pond at mouth of rio Preto (currently flooded by Cana Brava reservoir), 13°37′51″S, 48°07′01″W, D. F. Moraes, 3 December 1996; MZUSP 89546*, paratype, 1, 25.6 mm SL, rio Crixás-açu, Araguaia-Tocantins Dr., under bridge at highway GO-465, Crixás/Santa Terezinha de Goiás municipality, 14°26′26″S, 49°42′37″W, Equipe CBE, 28 July 2005.

Xyliphius barbatus Alonso de Arámburu and Arámburu, 1962: Argentina: MACN 6791, 44.5–93.5 mm SL, río Paraná medio, 35–45 m trawls, R/V *Ara Petrel*, August 1975; Chaco: MCNCH* (now closed), holotype (lost) of *X. lombarderoi* Risso and Risso, 1964, río Paraná, Riacho Barranqueras near Puerto Vilelas, ca. 27°29′S, 58°52′19″W, M. Gabardini, June 1964; Santa Fe: MLP 6798 (ex. 12-VII-60-26), holotype, 91.5 mm SL, MLP 2799 (ex. 29-V-40-56), paratype, 1, río Paraná, Rosario, ca. 32°56′S, 60°38.5′W. Paraguay: Nueva Asunción: MNRJ 39103 (1 alc), río Paraguay (main channel), near Asunción, 25°15′40″S, 57°38′8″W, G. Hellweg, 24 October 2011.

Xyliphius kryptos Taphorn and Lilyestrom, 1983: Colombia: Norte de Santander: IAvH-P-3085 (1 alc), río Zulia, Catatumbo Dr., San Calixto, 8°18′0″N, 72°26′24″W, no collector, no date. Venezuela: Mérida: CVULA V-2520*, paratype (1 alc), 106 mm SL, CVULA V-2521*, paratype, 1, 110 mm SL, río Chama, bridge at El Vigía, ca. 8°36′37″N, 71°37′53″W, E. Navidad et al., 13 December 1981; Trujillo: MCNG 27310 (2 alc, 1 CS), río Carache, Motatán-Maracaibo Dr., exact locality unknown, plotted at confluence with río Monay, 9°36′46.3″N, 70°33′20.4″W, 27 August 1990; Zulia: MCNG 1224, holotype, 87 mm SL, río Aricuaisá near rt. 6 bridge, 9°24′32.5″N, 72°36′25.3″W, D. Taphorn and C. Lilyestrom, 26 April 1977.

Xyliphius lepturus Orcés V., 1962: Ecuador: USNM 301688 (1 alc), Concepción, Alto Napo, J. Olalla, October–November 1956; Napo: FMNH 99486 (1 alc), río Aguarico at San Pablo Kantesiya, 0°15′18″S, 76°25′30″W, D. J. Stewart et al., 23 November 1983; FMNH 99488 (3 alc, 1 CS), río Napo, Amazonas Dr., at Anagu, middle of mainstream, 0°31′36″S, 76°22′54″W, D. J. Stewart et al., 12 October 1981; FMNH 99490 (1 alc), río Napo at Puerto Misahualli, 1°2′30″S, 77°39′12″W, M. C. Ibarra and R. Barriga, 7 November 1981; Orellana: IAvH-P 1625 (2 alc), río Napo below mouth of río Coca, Puerto Francisco de Orellana, ca. 0°28′17.8″S, 76°58′01.1″W, O. Pinto, 1987; Pastaza: Orcés pers. coll. 1307* (holotype, not found at MEPN), 2020* (paratype, 1 alc), MEPN 870–871* (paratypes, 1, 1 alc), 902 (paratype, 1 alc), río Pucayacu at confluence with rio Bobonaza, Pastaza-Marañon Dr., 1°54′21.4″S, 77°13′16.3″W. Colombia: Meta: ANSP 128940 (1 alc), río Metica, Meta Dr., approx. 1.5 km east of Rajote, ca. 3°55′10″N, 73°03′W, W. G. Saul et al., 19 March 1973; ANSP 128941 (1 alc), río Guayuriba, Meta Dr., sandy point and bare riffly area on N side of river about 3 km upstream from its mouth, ca. 3°55′39″N, 73°05′54″W, J. E. Böhlke et al., 23 February 1972. Peru: Amazonas: AUM 46757 (1 alc), río Marañon, 12 km north of Imacita, 4°56′54.9″S, 78°20′31.6″W, N. K. Lujan et al., 10 August 2006; MUSM 19195 (1 alc), río Marañon, Condorcanqui, 5°01′50″S, 78°19′56″W, M. Hildago, 26 September 2001; Huánuco: MUSM 608 (1 alc), río Pachitea, Pacanasi, Tournavista, 8°56′02.8″S, 74°42′29.4″W, H. Ortega, 9 August 1975; La Convención: MUSM 41658 (1 alc), río Urubamba, station H14 at Timpía, Echarate District, 12°04′38.5″S, 72°49′34.9″W, I. Sipión, 25 August 2011. Venezuela: Apure: MCNG 50542 (1 alc), río Apure, Isla del Medio near Boquerones, ca. 7°48′51.5″N, 67°21′33.7″W, O. Brull, 25 August 1988; MCNG 51107 (2 alc), río Apure toward mouth of rio Portuguesa, ca. 7°56′05.8″N, 67°32′16.2″W, F. Provenzano and O. Castillo, 31 May 1989; Portuguesa: MCNG 5547 (32 alc, 1 CS), MCNG 5549 (21 alc), río Boconó, Apure Dr., La Veguita, 8°50′42.0″N, 70°00′42.1″W, D. Taphorn et al., 6–7 November 1982; Tachira: MCNG 23114, 1, río Camburito, Apure Dr., at dam, 7.6931°N, 71.5403°W, Equipo CADAFE, 7 February 1990; MCNG 23517, 1, río Camburito, Apure Dr., dry margin approx. 1000 m below dam, 7.6889°N, 71.5361°W, Equipo CADAFE, 7 February 1990.

Xyliphius magdalenae Eigenmann, 1912: Colombia: Boyacá: IAvH-P 3277 (1 alc), río Guaguaqui, Puerto Boyacá, 5°42′0″N, 74°20′0″W, F. Rodriguez, 1994; Cundinamarca: FMNH 56039 (ex. CM 4829), holotype, 32 mm SL, río Magdalena, Giradot, ca. 4°17′17″N, 74°48′31″W; Tolima: CZUT 1288, 1, 72.9 mm SL, río Amoyá, ca. 3°40′12.3″N, 75°21′32.6″W, IAvH-P 4127, 1, 72.0 mm SL, río Magdalena, received from fishermen at Honda, M. Sabaj et al., 27 July 2006; USNM 120224 (2 alc), río Magdalena at Honda, C. Miles, January 1943.

Xyliphius melanopterus Orcés V., 1962: Brazil: Rondônia: UFRO-I 8925, 8928, río Madeira, Cachoeira de Jirau (near UHE Jirau), 9°19′40″S, 64°43′34″W. Colombia: Casanare: IAvH-P-3276 (1 alc), río Tocaría, Meta Dr., Yopal, 5°33′N, 72°13′W, V. Ortiz, 1994. Ecuador: Napo: FMNH 99493 (1 alc, 1 CS), río Aguarico, about 15–20 min. downriver from Destacamento Zancudo, 0°33′S, 75°27′W, D. J. Stewart et al., 27 October 1983; FMNH 99495 (3 alc), MZUSP 38679, 1, río Napo, Amazonas Dr., at Anagu, middle of mainstream, 0°31′36″S, 76°22′54″W, D. J. Stewart et al., 12 October 1981; Pastaza: Orcés pers. coll. 2021* (holotype, not found at MEPN), río Pucayacu near confluence with río Bobonaza, Pastaza-Marañon Dr., ca. 1°54′21.4″S, 77°13′16.3″W. Peru: Loreto: MUSM 4720 (1 alc), USNM 329607 (1 alc), río

Aguarico, Napo Dr., puesto de vigilancia Castaña, depth 6–9 m, cal. 0°51′02.7″S, 75°14′21.2″W, F. Chang and M. Hagedorn, 23–24 October 1993; Madre de Dios: MUSM 36715 (2 alc), río Las Piedras, below Santa Teresita, 12°30′29″S, 69°15′14″W, J. Albert et al., 24 May 2011; Ucayali: MUSM 40907 (3 alc), quebrada Popa, Purus Dr., Balta, 10°08′06.8″S, 71°05′51.5″W, D. Lopez, 22 January 2011. Venezuela: Portuguesa: MCNG 5548 (1 alc), río Boconó, La Veguita, Apure Dr., 8°50′42.0″N, 70°00′42.1″W, D. Taphorn et al., 7 November 1982; Tachira: MCNG 23518 (2 alc), río Camburito, Apure Dr., dry margin aprox. 1000 m below dam, 7.6889°N, 71.5361°W, Equipo CADAFE, 7 February 1990.

ACKNOWLEDGMENTS

For hosting museum visits and loans of specimens we thank C. McMahan and S. Mochel (FMNH); L. Rapp Py-Daniel (INPA); C. Oliveira and F. Roxo (LBP); O. Castillo (MCNG); C. Lucena (MCP); H. López, A. Miquelarena, and D. Nadalin (MLP); M. Britto and P. Buckup (MNRJ); H. Ortega and J. Espino (MUSM); A. Datovo, M. Gianetti, and O. Oyakawa (MZUSP); Ruth Reina (STRI); H. López-Fernández (ROM); S. Raredon and the late R. Vari (USNM). For additional data on museum specimens, thanks to C. DoNascimiento (IAvH-P), D. Taphorn (MCNG), M. Britto (MNRJ), C. Cramer (UFRO), R. Ota (INPA), and J. Espino and V. Meza (MUSM). Thanks to M. Azpelicueta for information on specimens studied by Risso and Risso, and A. Almendariz and R. Barriga for information specimens studied by Orcés. Thanks to M. Britto (MNRJ) for providing rare literature and X-ray images of *Xyliphius*. Thanks to WINS students T. Bell, G. Johnson, and F. Truong (ANSP) for preparing digital X-rays. Thanks also to J. García-Melo, M. Bernt, J. Espino, and A. Thomaz for photographs of *Xyliphius*. We thank J. Maisano and M. Colbert (UT Austin) for preparation of computed tomography X-rays and K. Luckenbill (ANSP) for help in image editing with VGStudio MAX software. The first author (TPC) thanks CNPq (process #229355/2013-7) for podsdoctoral fellowship and is currently supported by a PNPD-CAPES fellowship. The third author (RER) is supported by the Conselho Nacional de Desenvolvimento Científico e Tecnológico (CNPq process #306455/2014-5). Computed tomography supported by Fundação de Amparo à Pesquisa do Estado do Rio Grande do Sul–FAPERGS (2361-2551/14-7). Study supported by the All Catfish Species Inventory (NSF DEB-0315963) and iXingu Project (NSF DEB-1257813). Thanks to D. Faustino-Fuster for translating the abstract to Spanish. We thank A. Thomaz, B. Calegari, and M. Arce for help and guidance with molecular work. We also thank J. Lundberg and J. Friel for discussions on catfish morphology and river channel fishes.

LITERATURE CITED

Alonso de Arámburu, A. S., and R. H. Arámburu. 1962. Una nueva especie de *Xyliphius* de la Argentina (Siluriformes, Bunocephalidae). Physis 23:219–222.

Arce, H. M., R. E. Reis, A. J. Geneva, and M. H. Sabaj Pérez. 2013. Molecular phylogeny of thorny catfishes (Siluriformes: Doradidae). Molecular Phylogenetics and Evolution 67:560–577.

Calviño, P. A., and H. P. Castello. 2008. Sobre un bagre ciego del Río Paraná médio, *Xyliphius barbatus* Arámburu y Arámburu, 1962 (Siluriformes: Aspredinidae) uma nueva cita em la Argentina y comentarios adicionales. Lãs Ciências, Revista de la Universidad Maimónides 1:55–59.

Cardoso, A. R. 2008. Filogenia da família Aspredinidae Adams, 1854 e revisão taxonômica de Bunocephalinae Eigenmann and Eigenmann, 1888 (Teleostei: Siluriformes: Aspredinidae). Unpubl. Ph.D. diss., PUCRS, Porto Alegre.

Cardoso, A. R. 2010. *Bunocephalus erondinae*, a new species of banjo catfish from southern Brazil (Siluriformes: Aspredinidae). Neotropical Ichthyology 8:607–613.

Carvalho, T. P., and J. S. Albert. 2011. Redescription and phylogenetic position of the enigmatic Neotropical electric fish *Iracema caiana* Triques (Gymnotiformes: Rhamphichthyidae) using x-ray computed tomography. Neotropical Ichthyology 9:457–469.

Carvalho, T. P., A. R. Cardoso, J. P. Friel, and R. E. Reis. 2015. Two new species of the banjo catfish *Bunocephalus* Kner (Siluriformes: Aspredinidae) from the upper and middle rio São Francisco basins, Brazil. Neotropical Ichthyology 13:499–512.

Chakrabarty, P., M. Warren, L. M. Page, and C. C. Baldwin. 2013. GenSeq: an updated nomenclature and ranking for genetic sequences from type and non-type sources. ZooKeys 346:29–14.

Dahdul, W. M., P. M. Mabee, J. G. Lundberg, P. E. Midford, J. P. Balhoff, H. Lapp, T. Vision, M. A. Haendel, and M. Westerfield. 2010. The teleost anatomy ontology: anatomical representation for the genomics age. Systematic Biology 50:369–683.

Figueiredo, C. A., and M. R. Britto. 2010. A new species of *Xyliphius*, a rarely sampled banjo catfish (Siluriformes: Aspredinidae) from the rio Tocantins-Araguaia system. Neotropical Ichthyology 8:105–112.

Friel, J. P. 1994. A phylogenetic study of the Neotropical banjo catfishes (Teleostei: Siluriformes: Aspredinidae). Unpubl. Ph.D. diss., Duke University, Durham, North Carolina.

Friel, J. P. 1995. *Acanthobunocephalus nicoi*, a new genus and species of miniature banjo-catfish from the upper Orinoco and Casiquiare rivers, Venezuela (Siluriformes: Aspredinidae). Ichthylogical Exploration of Freshwaters 6:89–95.

Friel, J. P. 2003. Family Aspredinidae, p. 261–267. *In*: Check List of the Freshwater Fishes of South and Central America. R. E. Reis, S. O. Kullander, and C. J. Ferraris, Jr. (eds.). Edipucrs, Porto Alegre.

Friel, J. P., and T. P. Carvalho. 2016. A new species of *Amaralia* Fowler (Siluriformes: Aspredinidae) from the Paraná-Paraguay River Basin. Zootaxa 4088:531–546.

Friel, J. P., and J. G. Lundberg. 1996. *Micromyzon akamai*, gen. et sp. nov., a small and eyeless banjo catfish (Siluriformes: Aspredinidae) from the river channels of the lower Amazon basin. Copeia 1996:641–648.

Hilton, E. J., C. Cox Fernandes, J. P. Sullivan, J. G. Lundberg, and R. Campos-da-Paz. 2007. Redescription of *Orthosternachus tamandua* (Boulenger, 1898) (Gymnotiformes, Apteronotidae), with reviewes of its ecology, electric organ discharges, external morphology, osteology and phylogenetic affinities. Proceeding of the Academy of Natural Sciences of Philadelphia 156:1–25.

Herbert, P. D. N., A. Cywinska, S. Ball, and J. R. Dewaard. 2003. Biological identifications through DNA barcodes. Proceedings of Royal Society B: Biological Sciences 270: 313–321.

Ivanyisky, S. J., III, and J. S. Albert. 2014. Systematics and biogeography of Sternarchellini (Gymnotiformes: Apteronotidae): diversification of electric fishes in large Amazonian rivers. Neotropical Ichthyology 13:565–584.

Li, C., G. Ortí, G. Zhang, and G. Lu. 2007. A practical approach to phylogenomics: the phylogeny of ray-finned fish (Actinopterygii) as a case study. BMC Evolutionary Biology 7:44.

Lundberg, J. G., K. R. Luckenbill, K. K. Subhash Babu, and H. H. Ng. 2014. A tomographic osteology of the taxonomically puzzling catfish *Kryptoglanis shajii* (Silurifomes, Siluroidei, *incertae sedis*): description and a first phylogenetic interpretation. Proceedings of the Academy of Natural Sciences of Philadelphia 163:1–41.

Lundberg, J. P., and L. Rapp Py-Daniel. 1994. *Bathycetopsis oliveirai*, gen. et sp. nov., a blind and depigmented catfish (Siluriformes: Cetopsidae) from the Brazilian Amazon. Copeia 1994:381–390.

Maldonado-Ocampo, J. A., A. Ortega-Lara, J. S. Usma, G. Galvis, F. A. Villa-Navarro, L. Vasquez, S. Prada-Pedreros, and C. A. Ardila R. 2005. Peces de los Andes de Colombia: Guía de Campo. 1 ed. Instituto de Investigación de Recursos Biológicos Alexander von Humboldt, Bogotá, Colombia.

Mees, G. F. 1987. The member of the subfamily Aspredininae, family Aspredinidae in Suriname (Pisces, Nematognathi). Proceedings of the Koninklijke Nederlandse Akademie van Wetenschappen 90:173–192.

Mungall, C. J., C. Torniai, G. V. Gkoutos, S. E. Lewis, and M. A. Haendel. 2012. Uberon, an integrative multi-species anatomy ontology. Genome Biology 13:R5.

Ohara, W. M., and J. Zuanon. 2013. Aspredinidae, p. 108–141. *In:* Peixes do Rio Madeira L. J. Queiroz, G. Torrente-Vilara, W. M. Ohara, T. H. S. Pires, and J. Zuanon. São Paulo, Santo Antonio Energia.

Orcés, V. G. 1962. Dos nuevos peces del genero *Xyliphius*. Ciencias Naturales 5:50–54.

de Pinna, M. C. 1996. A phylogenetic analysis of the Asian catfish families Sisoridae, Akysidae, and Amblycipitidae, with hypothesis on the relationships of the Neotropical Aspredinidae (Teleostei, Ostariophysi). Fieldiana, Zoology 84:1–83.

Risso, F. J. J., and E. N. P. de Risso. 1964. Hallazgo de una nueva especie de *Xyliphius* en el Parana (Pisces–Aspredinidae). Notas del Museo de Ciencias Naturales del Chaco 1: 11–16.

Sabaj Pérez, M. H. 2009. Photographic atlas of fishes of Guiana Shield, p. 53–59. *In*: Checklist of the Freshwater Fishes of the Guiana Shield. R. P. Vari, C. J. Ferraris, A. Radosavljevic, and V. A. Funk (eds.). Bulletin of the Biological Society of Washington, Washington, D.C.

Sabaj Pérez, M. H. (Ed.). 2014. Standard symbolic codes for institutional resource collections in herpetology and ichthyology: an Online Reference. Version 5.0 (22 September 2014). Electronically accessible at http://www.asih.org/, American Society of Ichthyologists and Herpetologists, Washington, D.C.

Schaefer, S. A. 2003. Relationships of *Lithogenes villosus* Eigenmann, 1909 (Siluriformes, Loricariidae): evidence from high-resolution computed microtomography. American Museum Novitates 3401:1–55.

Schaefer, S. A., and L. Fernández. 2009. Redescription of the Pez Graso, *Rhizomichthys totae* (Trichomycteridae) of Lago Tota, Colombia, and aspects of cranial osteology revealed by microtomography. Copeia 2009:510–522.

Stewart, D. J., M. Ibarra, and R. Barriga-Salazar. 2002. Comparison of deep-river and adjacent sandy-beach fish assemblages in the Napo River Basin, eastern Ecuador. Copeia 2002:333–343.

Taphorn, D. C., and C. G. Lilyestrom. 1983. Un nuevo pez del genero *Xyliphius* (Aspredinidae) de Venezuela. Revista Unellez de Ciencia y Tecnología 1:43–44.

Taphorn, D. C., and C. Marrero. 1990. *Hoplomyzon sexpapilostoma*, a new species of Venezuelan catfish (Pisces: Aspredinidae), with comments on the Hoplomyzontini. Fieldiana, Zoology 61:1–9.

Taylor, W. R., and G. C. Van Dyke. 1985. Revised procedures for staining and clearing small fishes and other vertebrates for bone and cartilage study. Cybium 9:107–119.

Thomas, M. R., and L. H. Rapp Py-Daniel. 2008. Three new species of the armored catfish genus *Loricaria* (Siluriformes: Loricariidae) from river channels of the Amazon basin. Neotropical Ichthyology 6:379–394.